Consequences of human cytomegalovirus infection on small extracellular vesicles isolated from first trimester placental histocultures

Mathilde Bergamelli [1] *, Hélène Martin [1] *, Mélinda Bénard [1,2], Jérôme Ausseil [1,3], Jean-Michel Mansuy [4], Ilse Hurbain[5,6], Maïlys Mouysset [1], Marion Groussolles [1,7,8], Géraldine Cartron [9], Yann Tanguy le Gac [9], Nathalie Moinard [10], Elsa Suberbielle [1], Jacques Izopet [1,4], Charlotte Tscherning [1,‡], Graça Raposo [5,6], Daniel Gonzalez-Dunia [1], Gisela d'Angelo [5], and Cécile E. Malnou [1]#

[1] Centre de Physiopathologie Toulouse-Purpan (CPTP), Université de Toulouse, INSERM, CNRS, UPS, Toulouse, France.

[2] CHU Toulouse, Hôpital des Enfants, Service de Néonatalogie, Toulouse, France.

[3] CHU Toulouse, Hôpital Rangueil, Laboratoire de Biochimie, Toulouse, France.

[4] CHU Toulouse, Hôpital Purpan, Laboratoire de Virologie, Toulouse, France.

[5] Institut Curie, CNRS UMR144, Structure et Compartiments Membranaires, Université Paris Sciences et Lettres, Paris, France.

[6] Institut Curie, CNRS UMR144, Plateforme d'imagerie cellulaire et tissulaire (PICT-IBiSA), Université Paris Sciences et Lettres, Paris, France.

[7] CHU Toulouse, Hôpital Paule de Viguier, Service de Diagnostic Prénatal, Toulouse, France.

[8] Equipe SPHERE Epidémiologie et Analyses en Santé Publique: Risques, Maladies chroniques et handicaps, Université de Toulouse, INSERM UMR1027, UPS, Toulouse, France.

[9] CHU Toulouse, Hôpital Paule de Viguier, Service de Gynécologie Obstétrique, Toulouse, France.

[10] Groupe de Recherche en Fertilité Humaine (EA 3694), Université de Toulouse, Toulouse, France; CECOS, Groupe d'activité de médecine de la reproduction, CHU Toulouse, Hôpital Paule de Viguier, Toulouse, France.

[‡] Current address: Division of Neonatology, Sidra Medicine, Well-Cornell College, Doha, Qatar.

* These authors contributed equally to this work

Corresponding author

ABSTRACT

Currently, research on the use of non-invasive biomarkers as diagnosis and prognosis tools during pathological pregnancies is in full development. Among these, the placenta-derived small extracellular vesicles (sEVs) are considered as serious candidates. As such, their composition is modified during many pregnancy pathologies and they can be easily purified from a simple blood sample, as they are found in maternal serum. In this study, we describe the isolation of sEVs from a histoculture model of first trimester placental explants. We characterized these sEVs by a combination of biochemical, bead-based multiplex cytometry and electron microscopy approaches and defined their associated markers and ultrastructure. We next examined the consequences for sEVs secretion and characteristics of placenta infection by the human cytomegalovirus. Under these conditions, the secretion and integrity of sEVs was preserved. However, an increase in the expression level of several surface markers

was detected, opening up the prospect for the search for biomarkers predicting the severity and the outcome of this congenital infection early during the pregnancy, which are still sorely lacking.

Keywords: early placenta, extracellular vesicles, congenital infection, human cytomegalovirus, histoculture.

INTRODUCTION

Long considered as a passive barrier, the placenta is now clearly recognized to actively orchestrate the numerous exchanges between mother and fetus, in oxygen, nutrients and waste, protecting the fetus against infections and allowing adaptation of maternal metabolism to pregnancy [1, 2]. In the past decade, a new mode of communication of the placenta with both maternal and fetal sides has been described and extensively studied, consisting in the secretion of placental extracellular vesicles (EVs), which increases all along pregnancy and stops after delivery [3, 4]. EVs are membranous nanovesicles released by cells in the extracellular space and body fluids, under physiological and pathophysiological conditions [5, 6]. In a simplistic way, we can distinguish large microvesicles (up to 1 μm), derived from plasma membrane by direct outward budding, and exosomes, ranging from 30 to 200 nm of diameter, which are generated by inward budding of endosomal membrane before their release into the extracellular space. Discrimination between the different types of EVs based on their biogenesis pathway and/or physical characteristics is still the subject of intense work and numerous studies, and their classification is continuously evolving [5-8]. Hence, as it is often difficult to clearly prove the exact nature of exosomes compared to other vesicle

73 subtypes, the term exosome has sometimes been used improperly in the literature, which
74 must be interpreted with caution. We have therefore chosen in this manuscript to use the
75 terminology small EVs (sEVs), according to the ISEV guidelines [9].

76 Interestingly, placental sEVS are detected in the maternal serum during pregnancy and
77 their composition is altered upon placental pathologies, such as, amongst others, diabetes
78 mellitus, intrauterine growth restriction or preeclampsia [10-16]. Thus, sEVs may represent
79 precious non-invasive biomarkers reflecting the status of the placenta and of the pregnancy
80 [17, 18]. In order to identify such biomarkers for use in diagnosis or prognosis, it is important
81 to develop models close to the (patho)physiology allowing preparation of placental sEVs in a
82 robust and reproducible manner, guaranteeing their purity for downstream analysis. It is
83 especially the case for early placentas, since many pregnancy pathologies and developmental
84 defects are the result of placental insults occurring during the first trimester of pregnancy [19-
85 21]. In this regard, the use of tissue explant models is particularly relevant, since they preserve
86 the tissue cytoarchitecture, allowing to decipher the complex mechanism of
87 (patho)physiological processes [22, 23]. Finally, such models should endure chronic stressors,
88 to examine the effects of environmental insults on the secretion of sEVs over several days,
89 this aspect being particularly limiting in the currently available models.

90 Among many environmental agents, viral congenital infections are a major cause of
91 placental and fetal development impairments. Infection by the human cytomegalovirus
92 (hCMV) concerns 1% of live births in developed countries, and is responsible for various
93 placental and fetal damages, especially at the level of the fetal central nervous system, leading
94 to various brain disorders [24-26]. Non-invasive diagnostic tools to assess fetal infection by
95 hCMV are lacking, since the gold standard diagnosis is using PCR on amniotic fluid, resulting
96 in the necessity to perform an invasive amniocentesis, which is not devoid of risk [27].

97 Concerning prognosis, there are currently very few methods easily implementable to predict
98 fetal impairment, especially concerning neurosensorial damage [28-30]. Thus, the
99 identification of non-invasive diagnosis and prognosis biomarkers within sEVs would be a
100 great step forward in assessing placental and fetal damage and would provide a valuable
101 decision support tool.

102 In this context, we have adapted a histoculture model of first trimester placental
103 explants that was developed in our team [31, 32], in order to isolate sEVs with a purity
104 compatible with analyses of their composition and features. This model, permissive to hCMV
105 infection [31, 32], allowed us to purify sEVs devoid of contaminant viral particles. We showed
106 that the secretion and integrity of sEVs is preserved upon hCMV infection of placentals
107 explants, with significant modifications in the expression levels of some sEV surface proteins.
108 Thus, this model opens up immense prospects for modeling chronic stresses at the start of
109 pregnancy, like viral infections, to find biomarkers allowing to detect very early placental and
110 fetal damage.

111

112 **MATERIALS AND METHODS**

113

114 **Human ethic approval**

115 The Germethèque biological resource center at the Toulouse site (BB-0033-00081) provided
116 21 placenta samples in order to carry out the research program. Except term of pregnancy, no
117 other associated clinical data were collected in accordance with policy concerning voluntary
118 pregnancy termination. Germethèque obtained the agreement from each patient to use the
119 samples (CPP.2.15.27). The steering committee gave its agreement for the realization of this
120 study on 05/02/2019. The biological resource center has a declaration DC-2014-2202 and an

121 authorization AC-2015-2350. The hosting request made to Germethèque bears the number
122 20190201 and its contract is referenced under the number 19 155C.
123
124 **hCMV viral strain, viral stock production and titration**
125 The viral strain of hCMV used in this study is the endotheliotropic VHL/E strain (a kind gift from
126 C. Sinzger, University of Ulm, Germany) [33]. Viral stock was made by amplification of the virus
127 on MRC5 cells and concentration by ultracentrifugation, as described previously [34]. Virus
128 titration was determined by indirect immunofluorescence assays against the Immediate Early
129 (IE) antigen of hCMV upon infection of MCR5 by serial dilutions of the viral stock [34].
130 Additionally, virus titration was also performed by qPCR as described on viral stock and
131 placental histoculture supernatants [35].
132
133 **Placental histoculture and infection**
134 In order to purify sEVs from placental histocultures, culture media was depleted beforehand
135 from EVs [9]. To this purpose, Dulbecco's Modified Eagle Medium (DMEM with Glutamax,
136 Gibco) supplemented with 20 % Fetal Bovine Serum (FBS, Sigma-Aldrich) was ultracentrifuged
137 at 100,000 g for 16 hours at 4 °C and filtered at 0.2 µm (rotor SW32Ti, with maximal
138 acceleration and brake). "Exofree" medium was then obtained by a 1:1 dilution with DMEM
139 to reach 10 % FBS and addition of antibiotics at the following concentrations: 100 U/ml
140 penicillin - 100 µg/ml streptomycin (Gibco), 2,5µg/ml amphotericin B (Gibco) and 100µg/ml
141 normocin (Invivogen).
142 Placental histocultures were adapted from the model we previously described and validated
143 (Figure 1 A) [31, 32, 36]. First trimester placentas (mean = 11.72 ± 0.39 (SEM) weeks of
144 amenorrhea, *i.e.* 9.72 ± 0.39 weeks of pregnancy) were collected following elective abortions

145 by surgical aspiration at Paule de Viguier Maternity Hospital (Toulouse, France) by the medical
146 team. Isolation of trophoblastic villi was manually performed from total placental tissue with
147 particular care to exclude decidua, membranes and umbilical cord, by manual dissection in
148 Phosphate Buffer Saline (PBS). Tissues were washed in PBS until PBS cleared up, *i. e.,* upon
149 elimination of red blood cells. Each placenta was dissected in small pieces (2-3 mm^3) and kept
150 overnight in exofree medium in a 5 % CO_2 incubator at 37°C, to eliminate the remaining red
151 blood cells. To infect placental explants by hCMV upon dissection, the overnight incubation
152 was performed with 500µl of hCMV pure viral stock (corresponding to around 10^8 ffu) mixed
153 with 500µl of exofree medium. The day after (day 0), explants were washed six times in PBS
154 and installed, nine by nine, on re-hydrated gelatin sponges (Gelfoam, Pfizer) in a 6-well plate
155 containing 3 ml of exofree medium per well (Figure 1 A). A minimum of six wells, *i.e.* 54
156 explants, were used per experimental condition. Conditioned medium was collected and
157 totally replaced with fresh exofree medium every 3 to 4 days for the duration of the culture.
158 To maximize the recovery of sEV and obtain a rate production compatible with further
159 analyses, conditioned media were pooled and kept at 4°C until EV purification. At two time
160 points during culture, 300 µl of culture supernatant were also used to measure β-HCG rate
161 and evolution. Free β-HCG was measured on a COBAS system (Roche Diagnostics,
162 Switzerland), modular analytics E170, cobas e601 according to manufacturer protocol
163 (Application Code Number 033) and according to a published method [37]. In addition to β-
164 HCG dosage, release of virus by infected explants, indicating active viral replication, was
165 assessed by hCMV qPCR titration on supernatant, as described above [35].
166 At the end-point of the histoculture, total collected medium was used to perform sEV
167 isolation. Placental explants were weighted in order to normalize, calculate sEV yield and
168 define an appropriate resuspension volume upon sEV preparation. Three explants were used

169 to proceed to immuno-histochemistry analysis and the others were frozen at -80°C for further
170 analyses.
171
172 **Histochemistry and immuno-histochemistry**
173 Placental explants were fixed in formalin during 24 h at room temperature and embedded in
174 paraffin. Tissue sections (5 μm) were de-waxed using xylene and alcohol and epitope retrieval
175 was carried out using citrate buffer (pH 6) at 95°C during 20 min. Sections were re-hydrated
176 using TBS 0.01 % Tween 20 for 5 min and blocked with 2.5 % horse serum for 20 min.
177 Immunostainings were performed with the following antibodies: rabbit anti-Cytokeratin-7
178 (Genetex; 2 μg/mL), mouse anti-Vimentin (Santa-Cruz; 2 μg/mL) and mouse anti-placental
179 alkaline phosphatase (Biolegend; 1 μg/mL). Immunostaining for hCMV was performed, as
180 previously described [32], using a mouse monoclonal antibody directed against the hCMV IE
181 antigen (clone CH160, Abcam). Secondary antibody-coupled to biotin was then used prior to
182 Vectastain RTU elite ABC Reagent (Vector laboratories) and staining by diaminobenzidine
183 (DAB). Sections were finally counter-stained with hematoxylin. Image acquisition was
184 performed on a Leica DM4000B microscope or on a scanner Pannoramic 250 (3DHISTECH).
185
186 **Isolation of sEVs**
187 All steps were performed at 4 °C and PBS solution was filtered on a 0.22 μm filter. Procedures
188 were adapted from [38-40] according to ISEV guidelines [9] and are presented in Figure 2A.
189 From collected histoculture media, several differential centrifugations were carried out: a first
190 preclearing centrifugation for 30 min at 1,200 g to eliminate dead cells and large debris, a
191 second ultracentrifugation for 30 min at 12,000 g (rotor SW32Ti, with maximal acceleration
192 and brake) to eliminate large EVs (principally microvesicles), and a last ultracentrifugation of

193 the remaining supernatant for 1 hour at 100,000 g (Rotor SW32Ti, with maximal acceleration
194 and brake) allowed to pellet sEVs. The pellet was then resuspended either in 100 µl PBS or in
195 diluent C (Sigma) in order to stain the vesicles by the lipophilic dye PKH67 (Sigma) according
196 to the manufacturer instructions (5 min incubation; 1:1,000 dilution). sEVs were then
197 resuspended in a solution of 40 % iodixanol in sucrose and the last purification step was
198 carried out by ultracentrifugation on a discontinuous iodixanol/sucrose gradient (10 to 40 %
199 iodixanol) with deposition of the sEVs on the bottom of the tube, during 18 h at 100,000 g
200 (rotor SW41Ti, acceleration 5, no brake). The fractions 2+3 of the six fractions harvested,
201 corresponding to a density of, respectively, 1.086 and 1.116, were then pooled and washed in
202 25 ml PBS. After a last ultracentrifugation for 1 h at 100,000 g (Rotor SW32Ti, with maximal
203 acceleration and brake), the pellet was resuspended in PBS, in a volume proportional to the
204 weight of tissue (1 µl PBS per 1 mg tissue).
205 We submitted all relevant data of our experiments to the EV-TRACK knowledgebase (EV-
206 TRACK ID: EV200049) and obtained an EV-METRIC score of 100 % [41].
207
208 **sEV flow cytometry**
209 A Mascquant VYB Flow Cytometer (Myltenyi Biotec) was set up with Megamix-plus SSC FITC
210 (Biocytex Stago) calibration beads to standardize sEV measurements. Megamix-plus SSC beads
211 of variable diameters (160 nm, 200 nm, 240 nm and 500 nm) were separated depending on
212 size using SSC side scatter. A gating strategy was defined on 160 nm and 200 nm beads
213 populations to analyze events of size below 200 nm (Figure 2B).
214 sEV preparations, previously stained with PKH67 as described above, were diluted 1:200 in
215 filtered PBS and analyzed with the same parameters as those used for calibration beads.
216 Gating on events of size below 200 nm allowed count of sEVs and calculation of their

217 concentration for each preparation (Figure 2C). Each sample was analyzed twice. Data were
218 then analyzed with FlowJo software (BD).
219
220 **Nanoparticle tracking analysis**
221 sEV preparations were diluted 1:100 in filtered PBS (0.2 µm) and tracked using a NanoSight
222 LM10 (Marvern Pananalytical) equipped with a 405 nm laser. Videos were recorded three
223 times during 60 s for each sample at constant temperature (22°C) and analyzed with NTA
224 Software 2.0 (Malvern instruments Ltd). Data were analyzed with Excel and GraphPad Prism
225 (v8) softwares.
226
227 **Transmission electron microscopy and immunolabeling electron microscopy**
228 Procedures were performed essentially as described [42, 43].
229 For transmission electron microscopy (TEM), sEV preparations were loaded on copper
230 formvar/carbon coated grids (Ted Pella). Fixation was performed with 2 % paraformaldehyde
231 in 0.1 M phosphate buffer (pH 7.4), followed by a second fixation with PBS 1 % glutaraldehyde
232 in PBS. Samples were stained with 4 % uranyl acetate in methylcellulose.
233 For immunolabeling electron microscopy (IEM), sEV preparations were loaded on grids and
234 fixed with 2 % paraformaldehyde in 0.1 M phosphate buffer (pH 7.4). Immunodetection was
235 performed with a mouse anti-human CD63 primary antibody (Abcam ab23792). Secondary
236 incubation was next performed with a rabbit anti mouse Fc fragment (Dako Agilent Z0412).
237 Grids were incubated with Protein A-Gold 10 nm (Cell Microscopy Center, Department of Cell
238 Biology, Utrecht University). A second fixation step with 1 % glutaraldehyde in PBS was
239 performed. Grids were stained with uranyl acetate in methylcellulose.

240 All samples were examined with a Tecnai Spirit electron microscope (FEI, Eindhoven, The
241 Netherlands), and digital acquisitions were made with a numeric 4k CCD camera (Quemesa,
242 Olympus, Münster, Germany). Images were analysed with iTEM software (EMSIS) and
243 statistical studies were done with Prism-GraphPad Prism software (v8).
244
245 **Multiplex bead-based flow cytometry assay**
246 sEV preparations were subjected to bead-based multiplex EV analysis by flow cytometry using
247 the MACSPlex Exosome Kit, human (Miltenyi Biotec), according to the manufacturer
248 instructions [44].
249 Briefly, sEV preparations were incubated overnight with 39 different bead populations, each
250 coupled to a different capture antibody. The different bead populations are distinguishable
251 by flow cytometry by a specific PE and FITC labeling. sEVs bound to the beads were then
252 detected with a cocktail composed by anti-CD63, anti-CD9 and anti-CD81 antibodies coupled
253 to APC. Beads coupled to isotype control antibodies were used to assess potential non-specific
254 binding of sEVs. Background was also defined by performing the analysis without any sEVs.
255 Flow cytometry analysis was performed with a MACSQuant Analyzer 10 flow cytometer
256 (Miltenyi Biotec). The tool MACSQuantify was used to analyze flow cytometry data
257 (v2.11.1746.19438). The background signals were subtracted from the signals obtained for
258 beads incubated with sEVs. GraphPad Prism (v8) software was used to perform statistical
259 analysis of the data.
260
261 **Western blot**
262 sEV samples were lysed in non-reducing conditions in Laemmli buffer, heated for 5 min at 95
263 °C, and loaded on mini protean TGX precast 4-20 % gradient gels (Biorad) in tris-glycine buffer

264 for electrophoresis at 110 V for 2 h. Proteins were electro-transferred onto nitrocellulose
265 membranes using the trans-blot turbo transfer system (Biorad) and membranes were blocked
266 with Odyssey blocking buffer (Li-Cor Biosciences) for 1 h. Membranes were then incubated
267 with primary antibodies: mouse anti-CD81 (200 ng/ml, Santa-Cruz), mouse anti-CD63 (500
268 ng/ml, BD Pharmingen) or mouse anti-CD9 (100 ng/ml, Millipore) overnight at 4 °C in Odyssey
269 blocking buffer, followed by incubation with the secondary antibody IRDye 700 goat anti-
270 mouse IgG (Li-Cor Biosciences), for 1 h at room temperature. Membranes were washed three
271 times in TBS 0.1 % Tween 20 during 10 min after each incubation step and visualized using the
272 Odyssey Infrared Imaging System (LI-COR Biosciences).
273
274 **RESULTS**
275
276 In order to isolate sEVs and standardize their production from placental tissue, we
277 adapted the placental histoculture protocol already developed and characterized by our team
278 [31, 32]. To this aim, first trimester placentas (mean = 11.72 ± 0.39 (SEM) weeks of
279 amenorrhea; *i.e.* 9.72 ± 0.39 weeks of pregnancy) were obtained upon voluntary pregnancy
280 termination and cultured as described in Materials and Methods section, in exofree medium.
281 Culture supernatant was collected and renewed according to standardized time frame (Figure
282 1A). At the end of the culture (at day 14 or 15, exceptionally longer), placental explants were
283 collected and weighted for normalization. At two different time-points after the beginning of
284 culture, a sample of culture medium was subjected to β-HCG dosage to assess the viability of
285 the placental explants [45]. As indicated in Figure 1B, placental explants secreted β-HCG at
286 high levels, with a decrease with time, but which remains sustained and important (Measure
287 1, corresponding to β-HCG secreted between day 0 and 4: mean = 11,127 ± 1,699 mUI/ml;

288 Measure 2, corresponding to β-HCG secreted between day 7 and 11: mean = 2,478 ± 500
289 mUI/ml), similarly to our previous data [31]. Finally, evaluation of tissue architecture and
290 integrity was performed at the end of the culture by histochemistry and
291 immunohistochemistry. Tissue sections were examined for their expression of Cytokeratin-7
292 (CK-7; trophoblast marker), placental alkaline phosphatase (PLAP; syncitiotrophoblast marker)
293 and Vimentin (mesenchymal cell marker). The typical double layer of trophoblastic cells,
294 consisting of an outer syncitiotrophoblastic layer and an inner cytotrophoblastic layer, was
295 observed and surrounded the villous stroma (Figure 1D). These results indicated that
296 trophoblastic villi architecture was well preserved during the culture (Figure 1D) as we already
297 shown in previous works [31, 32].

298 To maximize the recovery of sEVs and allow their characterization, sEVs were prepared
299 from collected culture media pooled along the duration of the culture. For sEVS isolation,
300 differential ultracentrifugation steps and a final density ultracentrifugation on
301 Optiprep/sucrose gradient were combined (Figure 2A). Upon gradient ultracentrifugation, the
302 majority of sEVs was found into fractions 2 and 3, corresponding to a density of, respectively,
303 1.086 and 1.116, consistent with the density expected for sEVs [8, 38]. These fractions were
304 then pooled before a final ultracentrifugation step. The sEV pellet was then resuspended into
305 a final volume of PBS proportional to tissue weight for each experimental point, to allow the
306 normalization and comparison of sEV yield between experiments. Except when preparations
307 were intended to be used for multiplex bead-based flow cytometry assay, sEVs were
308 otherwise stained with the fluorescent lipophilic dye PKH67 before gradient
309 ultracentrifugation, to allow their counting by flow cytometry (Figure 2A). Flow cytometer was
310 calibrated with FITC-fluorescent beads of different sizes to define gating parameters before
311 analysis of sEV preparations (Figure 2B). Only vesicles of less than 200 nm of diameter were

312 counted; the majority of the analyzed events displayed an approximal size of less than 160 nm
313 (Figure 2C). The yields of sEVs were then calculated and normalized on the tissue weight. An
314 average yield of 29,459 ± 5,370 sEV/mg of tissue (mean ± SEM) was obtained when measured
315 by flow cytometry.

316 To further describe the population of purified sEVs, the approach of nanoparticle
317 tracking analysis (NTA) was used. Four independent sEV preparations were analyzed in
318 triplicate. Concentrations of sEVs determined for the four preparations lied in the same range
319 than the concentrations determined by flow cytometry and the comparison of the results
320 obtained by the two methods showed no significant difference (Supplementary Table 1). The
321 mode sizes for the four sEV preparations determined by NTA ranged between 125.7 and 170.7
322 nm, with a mean of 145.8 ± 9.3 nm (Figure 3A). In further details, the size distributions of two
323 of the sEV preparations showed small differences, as illustrated in Figures 3B and C, with only
324 slight peaks variations found at higher size, that may indicate the presence of aggregated
325 vesicles or contaminant microvesicles.

326 Next, an exhaustive morphological characterization of placental sEVs by TEM and IEM
327 was performed (Figure 4). This approach enables the analysis of membranous sEV and their
328 relative sizes with the selection of EV-like particles only, allowing the exclusion of aggregates
329 or of non-EV structures from the analysis. The preparations were highly enriched in vesicles
330 that presented the typical membranous appearance of sEVs (Supplementary Figure 1 and
331 Figure 4A). The average sEV size was then determined on isolated sEVs on two independent
332 sEV preparations. By this approach, determination is relative since the fixation and embedding
333 steps for the preparation of sEVs provoke shrinking of the vesicles. By focusing only on
334 selected sEVs according to their structures, average sizes obtained were 97 and 91 nm of
335 diameter for the two preparations (Figure 4B). More precisely, by observing sEV size

336 distribution, the majority of sEV diameters lied around 80 nm (Figure 4C). IEM allowing to
337 detect the canonical tetraspanin CD63, known to be enriched in endosome-derived exosomes,
338 was then performed. As observed in Figure 4D (and in Supplementary Figure 2), the majority
339 of sEVs were highly positive for CD63. A manual counting of CD63-positive sEVs among total
340 sEVs indicated that the percentage of CD63-positive sEVs was, respectively, of 60.32 and 61.83
341 % for the two sEV preparations.

342 Second, a multiplex bead-based flow cytometry assay was carried out to establish an
343 exhaustive map of sEV surface markers (Figure 5). To this aim, we used an assay that allows
344 for the simultaneous detection of up to 37 different EV surface markers in a semi-quantitative
345 way [44, 46]. As shown in Figure 5A and expected from the IEM results, a highly positive signal
346 for CD63, a canonical exosome surface protein, was observed, which was also detected by
347 western blot, as shown for two independent sEV preparations (Figure 5B). Two other
348 canonical sEV surface proteins, CD9 and CD81, were found expressed in the sEV preparations
349 (Figure 5A), but were not detected by western blot, probably because of the detection limit
350 of the antibodies (data not shown). Altogether, these data indicated that isolated sEVs showed
351 the typical features of canonical exosomes, regarding ultrastructure, size and presence typical
352 exosome markers.

353 This bead-based flow cytometry assay also showed the expression on sEV surface of
354 proteins expressed by trophoblastic cells like CD24 (already described on trophoblastic EVs)
355 [47], CD49e (also known as integrin α5) [48], CD105 [49], CD146 (also named MCAM) [50] or
356 CD236 (also known as EpCAM) [51]. Conversely, no expression of non-trophoblastic markers
357 was detected on sEVs preparations, like CD4, CD8, CD31, CD45 or HLA-ABC [48, 52]. Of note,
358 markers described for placental mesenchymal stem cells were also found at the surface of

359 isolated sEV like CD29 (also known as integrin β1), CD44 and SSEA-4 [53, 54], indicating that
360 these cells may also contribute to the sEV secretion of our model.

361 Next, the impact of the hCMV infection on the secretion and characteristics of
362 placental sEVs was examined. To this aim, placental explants were infected by the VHL/E
363 clinical strain overnight after tissue dissection, extensively washed and maintained in culture
364 during two weeks to let the virus disseminate, as already described by our team [31]. The
365 presence of virus release into the culture medium was monitored. To this end, one aliquot of
366 histoculture supernatant was taken after two medium renewals (corresponding to virus
367 released between days 7 and 11) and analyzed by qPCR. Upon infection, placental explants
368 displayed an active viral release, with hCMV titers in supernatant comprised between $1.05\ 10^4$
369 and $1.53\ 10^7$ copies/ml, the median lying at $3.04\ 10^5$ copies/ml (Figure 6A). Virus quantified in
370 the supernatant did not correspond to remaining inoculum, since no viral genome was
371 detected by qPCR on control experiments performed with UV-irradiated virus (data not
372 shown). At the end of the culture, analysis of the tissue sections by immunohistochemistry
373 allowed to verify the presence of the IE viral antigen (Figure 6B). Some cells showed intense
374 staining, demonstrating that the virus had disseminated well into the tissue after two weeks.
375 Viral infection did not modify the weight of tissue upon culture compared to non-infected
376 conditions (Figure 6C), neither the level of secreted β-HCG that remained similar between
377 non-infected and infected placentas for both measures 1 and 2 (Figure 6D). Finally, the tissue
378 architecture remained well preserved as attested by immunohistochemistry performed
379 against CK-7, PLAP and Vimentin (Figure 6E), thereby guaranteeing that the sEV preparations
380 were valuable and did not correspond to sEVs isolated from dying tissues that may lead to
381 misinterpretation of the results.

382 Finally, the characteristics of the sEVs secreted by non-infected or infected placental
383 histocultures were compared. The protocol for sEV preparation, combining differential
384 ultracentrifugation and gradient ultracentrifugation, was used to guarantee that viral particles
385 did not contaminate sEV preparation, as it has been described previously [40]. Indeed, hCMV
386 particles are bigger and denser than sEVs and should not be co-purified with sEVs with density
387 gradient ultracentrifugation [40]. The absence of infectious viral particles in sEV fractions was
388 effectively confirmed, by applying sEVs purified from infected placental explants to MCR5 cells
389 and performing an anti-IE immunofluorescence assay. As expected, no IE expression was
390 detected (Supplementary Figure 3). Moreover, no viral particle was detected by TEM in sEV
391 preparations in all the wide field pictures examined (exemplified in Supplementary Figure 4).
392 The yield of purified sEVs in non-infected *versus* infected histocultures was then
393 compared. No significant difference between the two conditions was observed (Figure 7A),
394 indicating that hCMV infection did not impact the global production of sEV by placental tissue.
395 By TEM, sEVs prepared from infected explants displayed the same morphology (Figure 7C and
396 Supplementary Figure 4) and relative size distribution compared to sEVs isolated from non-
397 infected histocultures (Figure 7D), with no significant difference in their mean size (Figure 7E).
398 sEVs prepared from hCMV-infected explants also expressed CD63, that was detected both by
399 western blot (Figure 7B) and by IEM (Figure 7F-G and Supplementary Figure 5), being
400 expressed on nearly 60% of the vesicles (Figure 7H).
401 Finally, the surface expression levels of several proteins expressed by sEVs were
402 examined by multiplex bead-based flow cytometry assay in both conditions (Figure 7I). To
403 perform this assay, quantification of the sEVs by PKH67-based flow cytometry upon sEV
404 preparation could not be realized, since it would interfere with the assay. Thus, sEV quantity
405 was normalized between non-infected and infected conditions based on the weight of the

406 explants, since the hCMV infection did not impact on the yield of sEV secretion (Figure 7A).
407 sEVs isolated from hCMV infected explants expressed the same markers as sEVs isolated from
408 non-infected explants, but with a significant different level of expression upon infection for
409 some of the markers (Figure 7I). A 2-way ANOVA statistical test confirmed that the infection
410 modified the global pattern of expression of sEV surface proteins (*p<0.0001* for the "Infection"
411 factor, no interaction with "Marker" factor). Most of the surface markers expressed in sEV
412 isolated from infected explants showed an increased expression upon infection. Bonferroni's
413 multiple comparison test indicated that two markers were significantly increased: CD81
414 (*p=0,0223*) and CD326 (EpCAM; *p=0,0029*). In conclusion, our results indicate that hCMV
415 infection of placental explants preserves the global secretion of sEVs that conserve the typical
416 characteristics of exosomes, with an increase in the expression levels of some surface proteins
417 that may be candidates as sEV markers of hCMV infection.
418
419 **DISCUSSION**
420
421 An increasing number of works aim to study placental EVs and their role in
422 physiological and pathological pregnancy. To this purpose, several models have been used as
423 a source of EVs, both *in vivo*, *ex vivo* or *in vitro*. *In vivo*, study of placental EVs isolated from
424 blood is hard to interpret because they come from multiple tissues. The use of placental
425 primary cells or cell lines *in vitro* is very informative but may lack important aspects of
426 (patho)physiology occuring in a complex tissue architecture, especially during viral infection.
427 Here we adapted a previously established model of first trimester placental explants,
428 maintained in culture at the air/liquid interface, and permissive for hCMV replication [31, 32].
429 This model, which has also been used by other teams for different types of tissues [22],

430 including placenta [23, 55, 56] allows the maintenance of the tissue in culture for several days.
431 In this study, we confirmed that the integrity of the placental explants was preserved,
432 consistent with our previous results [31, 32], with a still sustained, while decreased, secretion
433 of β-HCG along the culture, indicating the viability of the tissue [45]. Moreover, different
434 immunohistochemistry staining showed that the complex cytoarchitecture of the
435 trophoblastic villi was well preserved at the end of the culture, even upon hCMV infection.

436 From these placental explants, we developed robust and reproducible conditions for
437 the recovery and isolation of sEVs, by a combination of successive differential and density
438 gradient ultracentrifugation steps, adapted from [38-40] and in strict accordance with MISEV
439 guidelines [9]. This allows to obtain pure sEV preparations devoid of contaminants, as
440 evidenced by the various characterizations that were next carried out and the EV-METRIC
441 score of 100% [41]. The different characterizations performed on sEV preparations showed
442 that they present many features of endosomal-derived exosomes, including membranous
443 vesicles as observed by TEM, an average relative diameter around 95 nm and the presence of
444 exosome components including CD63, CD9 and CD81. Since the subcellular origin of these
445 vesicles cannot, however, be definitively ruled on, we have therefore chosen to keep the
446 designation of sEVs in this manuscript [9].

447 While in some studies, the authors focus their analysis on EVs isolated from a single
448 cell type, here the global population of sEVs secreted from trophoblastic villi was examined.
449 The origin of the vesicles is therefore varied, reflecting those of the placental environment,
450 which allows to assess the overall changes of the vesicles following stress. As the tissue
451 architecture was well preserved, it is likely that the outer layers of cyto- and
452 syncitiotrophoblasts are prone to mostly contribute to the sEV secretion observed, and
453 proteins expressed by trophoblasts were effectively detected, like CD326, CD24 or CD49e, on

454 the sEV surface [47, 48, 51]. The presence of proteins described for mesenchymal stem cells
455 was also observed, like CD29, CD44 and SSEA-4, indicating that such cells also probably
456 participate to the secretion of sEV in our model [53, 57]. Of note, even if sEV have different
457 cell origin, the pattern of expression of surface markers is very reproducible amongst sEV
458 preparations.

459 In this study, the sEVs secreted by the placental villi during infection by hCMV were
460 examined. To our knowledge, this is the first model that allows the isolation of sEVs from first
461 trimester placenta in the context of the hCMV infection. This virus is characterized by a
462 dissemination from the mother to the fetus *via* an active replication in the placenta tissue [58,
463 59]. Consistent with previous works [31, 32, 56, 60], the virus disseminated in the placental
464 explants during the culture, and was produced and released into the medium. Based on
465 immunohistochemistry data, tissue infection levels observed were similar to what can be
466 observed on placentas during natural infection [61]. Under our conditions of infection, the
467 placental explants kept the same weight and histological structure, and continued to secrete
468 sEVs, at yields comparable to the uninfected explants. The challenge of preparing sEVs in the
469 context of viral infections is to purify sEVs without being contaminated by viral particles, which
470 have physicochemical characteristics similar to sEVs [40, 62, 63]. In the case of hCMV, the size
471 and density characteristics of the viral particles, with a diameter of the order of 150 to 180
472 nm and a higher density than EVs, make possible their elimination from the sEV preparation
473 thanks to the density gradient ultracentrifugation step [40]. We indeed confirmed that sEV
474 preparations were devoid of infectious virus particles, and that no viral structure could be
475 detected by TEM in the numerous fields examined.

476 To maximize the recovery of sEVs and allow their characterization in downstream
477 analyses, especially during a slow rate infection like by hCMV, the histoculture supernatants

478 were pooled along the culture. This may be a limitation for the sEV analysis, since it could hide
479 fluctuations or attenuate transient or late trends induced by the virus. However, a significant
480 change in the sEV surface marker signature was observed upon infection of placental explants,
481 with a modification of global expression level of several surface proteins. A significant surface
482 expression increase was observed notably for two proteins: CD81 and CD326. Of note, CD326
483 (EpCAM) has been suggested to play a role in placental development [51, 64] and CD81 has
484 been recently described to play a role in hCMV entry [65, 66], but this was not demonstrated
485 for placental cells. Hence, it is tempting to speculate that the secretion of sEVs with this
486 specific pattern upon hCMV infection may have a functional role, by influencing viral
487 dissemination into the tissue and/or contributing to placental defects.

488 Currently, there is a growing interest for the search for biomarkers reflecting the state
489 of the placenta, even of the fetus, within the placental sEVs [14, 16-18]. However, in numerous
490 models of placental explants described to date, sEVs were generally prepared within the first
491 16 to 48 hours of culture, a duration that does not allow to evaluate the long-term effects of
492 chronic stress. Hence, this model of early placental explants cultured over several days is a
493 valuable tool to evaluate the impact of chronic environmental stress, as viral infection but also
494 hypoxia or endocrine disruptors, on the secretion and composition of sEVs secreted by the
495 placenta in early pregnancy, and opens new perspectives in the search for biomarkers.

496

497 **ACKNOWLEDGMENTS**

498

499 We thank the medical and paramedical staff of the gynecology unit at Paule de Viguier
500 Hospital, who allowed us to have access to the samples, as well as the patients who agreed to
501 participate in the study. We also warmly thank Louis Bujan and Mélanie Aubry, from the

Germethèque, for their help and professionalism, and Christian Sinzger who kindly provided us with the hCMV strain and gave us precious advice for its production. We greatly thank Benjamin Rauwel, Maryse Romao, Catherine Mengelle, Francine Chauvrier, Philippe Verdy, Nicolas Kopf and Matthieu Barbet, as well as the whole ViNeDys team, for their technical assistance and their numerous advices and discussions which allowed the progress of this work. Our thanks also go to Anne-Laure Iscache, Valérie Duplan-Eche and Fatima L'Faqihi-Olive, from the cytometry facility of the Center for Pathophysiology of Toulouse Purpan, as well as to Florence Capilla and Annie Alloy, from the histology facility Gentoul Anexplo. We also thank Laurence Nieto and Evert Haanappel from the Institute of Pharmacology and Structural Biology, who allowed us to have access to the Nanosight device, and for their many advices.

This project has received financial support from the French Society of Neonatology, the French Biomedicine Agency, the Réseau Mère-Enfant de la Francophonie. Our work was also financially supported by institutional grants from Inserm, CNRS and Toulouse 3 University. This project is part of the doctorate thesis of Mathilde Bergamelli, who was funded by the Ministry of Education and Research (MESR). The TEM experiments were performed on PICT-IBiSA, Institut Curie, Paris, member of the France-BioImaging national research infrastructure, and were supported by the French National Research Agency through the "Investments for the Future" program (France-BioImaging, ANR-11-INSB-04), supported by the CelTisPhyBio Labex (N° ANR-11-LB0038) part of the IDEX PSL (N°ANR-10-IDEX-0001-02 PSL).

DISCLOSURE STATEMENT

The authors report no conflict of interest.

526 **REFERENCES**

527 1. McNanley, T. and J. Woods, *Placental physiology.* Glob. libr. women's med., 2008.

528 2. Burton, G.J. and A.L. Fowden, *The placenta: a multifaceted, transient organ.* Philos Trans R Soc Lond
529 B Biol Sci, 2015. **370**(1663): p. 20140066.

530 3. Luo, S.S., et al., *Human villous trophoblasts express and secrete placenta-specific microRNAs into*
531 *maternal circulation via exosomes.* Biol Reprod, 2009. **81**(4): p. 717-29.

532 4. Sarker, S., et al., *Placenta-derived exosomes continuously increase in maternal circulation over the*
533 *first trimester of pregnancy.* J Transl Med, 2014. **12**: p. 204.

534 5. van Niel, G., G. D'Angelo, and G. Raposo, *Shedding light on the cell biology of extracellular vesicles.*
535 Nat Rev Mol Cell Biol, 2018. **19**(4): p. 213-228.

536 6. Kalluri, R. and V.S. LeBleu, *The biology, function, and biomedical applications of exosomes.* Science,
537 2020. **367**(6478).

538 7. Colombo, M., G. Raposo, and C. Thery, *Biogenesis, secretion, and intercellular interactions of*
539 *exosomes and other extracellular vesicles.* Annu Rev Cell Dev Biol, 2014. **30**: p. 255-89.

540 8. Kowal, J., et al., *Proteomic comparison defines novel markers to characterize heterogeneous*
541 *populations of extracellular vesicle subtypes.* Proc Natl Acad Sci U S A, 2016. **113**(8): p. E968-77.

542 9. Thery, C., et al., *Minimal information for studies of extracellular vesicles 2018 (MISEV2018): a*
543 *position statement of the International Society for Extracellular Vesicles and update of the*
544 *MISEV2014 guidelines.* J Extracell Vesicles, 2018. **7**(1): p. 1535750.

545 10. Salomon, C., et al., *Gestational Diabetes Mellitus Is Associated With Changes in the Concentration*
546 *and Bioactivity of Placenta-Derived Exosomes in Maternal Circulation Across Gestation.* Diabetes,
547 2016. **65**(3): p. 598-609.

548 11. Kandzija, N., et al., *Placental extracellular vesicles express active dipeptidyl peptidase IV; levels are*
549 *increased in gestational diabetes mellitus.* J Extracell Vesicles, 2019. **8**(1): p. 1617000.

550 12. Miranda, J., et al., *Placental exosomes profile in maternal and fetal circulation in intrauterine*
551 *growth restriction - Liquid biopsies to monitoring fetal growth.* Placenta, 2018. **64**: p. 34-43.

552 13. Chiarello, D.I., et al., *Foetoplacental communication via extracellular vesicles in normal pregnancy*
553 *and preeclampsia.* Mol Aspects Med, 2018. **60**: p. 69-80.
554 14. Cuffe, J.S.M., et al., *Review: Placental derived biomarkers of pregnancy disorders.* Placenta, 2017.
555 **54**: p. 104-110.
556 15. Herrera-Van Oostdam, A.S., et al., *Placental exosomes viewed from an 'omics' perspective:*
557 *implications for gestational diabetes biomarkers identification.* Biomark Med, 2019. **13**(8): p. 675-
558 684.
559 16. Malnou, E.C., et al., *Imprinted MicroRNA Gene Clusters in the Evolution, Development, and*
560 *Functions of Mammalian Placenta.* Front Genet, 2019. **9**: p. 706.
561 17. Mitchell, M.D., et al., *Placental exosomes in normal and complicated pregnancy.* Am J Obstet
562 Gynecol, 2015. **213**(4 Suppl): p. S173-81.
563 18. Jin, J. and R. Menon, *Placental exosomes: A proxy to understand pregnancy complications.* Am J
564 Reprod Immunol, 2018. **79**(5): p. e12788.
565 19. O'Tierney-Ginn, P.F. and G.E. Lash, *Beyond pregnancy: modulation of trophoblast invasion and its*
566 *consequences for fetal growth and long-term children's health.* J Reprod Immunol, 2014. **104-105**:
567 p. 37-42.
568 20. Silasi, M., et al., *Viral infections during pregnancy.* Am J Reprod Immunol, 2015. **73**(3): p. 199-213.
569 21. Montiel, J.F., H. Kaune, and M. Maliqueo, *Maternal-fetal unit interactions and eutherian*
570 *neocortical development and evolution.* Front Neuroanat, 2013. **7**: p. 22.
571 22. Grivel, J.C. and L. Margolis, *Use of human tissue explants to study human infectious agents.* Nat
572 Protoc, 2009. **4**(2): p. 256-69.
573 23. Fitzgerald, W., et al., *Extracellular vesicles generated by placental tissues ex vivo: A transport*
574 *system for immune mediators and growth factors.* Am J Reprod Immunol, 2018. **80**(1): p. e12860.
575 24. Cannon, M.J., D.S. Schmid, and T.B. Hyde, *Review of cytomegalovirus seroprevalence and*
576 *demographic characteristics associated with infection.* Rev Med Virol, 2010. **20**(4): p. 202-13.
577 25. Kenneson, A. and M.J. Cannon, *Review and meta-analysis of the epidemiology of congenital*
578 *cytomegalovirus (CMV) infection.* Rev Med Virol, 2007. **17**(4): p. 253-76.

579 26. Lanzieri, T.M., et al., *Seroprevalence of cytomegalovirus among children 1 to 5 years of age in the*
580 *United States from the National Health and Nutrition Examination Survey of 2011 to 2012.* Clin
581 Vaccine Immunol, 2015. **22**(2): p. 245-7.
582 27. Leruez-Ville, M., et al., *Cytomegalovirus infection during pregnancy: state of the science.* Am J
583 Obstet Gynecol, 2020. **223**(3): p. 330-349.
584 28. Leruez-Ville, M. and Y. Ville, *Fetal cytomegalovirus infection.* Best Pract Res Clin Obstet Gynaecol,
585 2017. **38**: p. 97-107.
586 29. Benoist, G., et al., *Cytomegalovirus-related fetal brain lesions: comparison between targeted*
587 *ultrasound examination and magnetic resonance imaging*. Ultrasound Obstet Gynecol, 2008. **32**(7):
588 p. 900-5.
589 30. Guerra, B., et al., *Ultrasound prediction of symptomatic congenital cytomegalovirus infection.* Am
590 J Obstet Gynecol, 2008. **198**(4): p. 380 e1-7.
591 31. Lopez, H., et al., *Novel model of placental tissue explants infected by cytomegalovirus reveals*
592 *different permissiveness in early and term placentae and inhibition of indoleamine 2,3-dioxygenase*
593 *activity.* Placenta, 2011. **32**(7): p. 522-30.
594 32. Benard, M., et al., *Human cytomegalovirus infection induces leukotriene B4 and 5-lipoxygenase*
595 *expression in human placentae and umbilical vein endothelial cells.* Placenta, 2014. **35**(6): p. 345-
596 50.
597 33. Stegmann, C., et al., *The N Terminus of Human Cytomegalovirus Glycoprotein O Is Important for*
598 *Binding to the Cellular Receptor PDGFRalpha.* J Virol, 2019. **93**(11).
599 34. Rolland, M., et al., *PPARgamma Is Activated during Congenital Cytomegalovirus Infection and*
600 *Inhibits Neuronogenesis from Human Neural Stem Cells.* PLoS Pathog, 2016. **12**(4): p. e1005547.
601 35. Mengelle, C., et al., *Performance of a completely automated system for monitoring CMV DNA in*
602 *plasma.* J Clin Virol, 2016. **79**: p. 25-31.
603 36. Rauwel, B., et al., *Activation of peroxisome proliferator-activated receptor gamma by human*
604 *cytomegalovirus for de novo replication impairs migration and invasiveness of cytotrophoblasts*
605 *from early placentas.* J Virol, 2010. **84**(6): p. 2946-54.

606 37. Sturgeon, C.M. and E.J. McAllister, *Analysis of hCG: clinical applications and assay requirements.*
607 Ann Clin Biochem, 1998. **35 (Pt 4)**: p. 460-91.
608 38. Ouyang, Y., et al., *Isolation of human trophoblastic extracellular vesicles and characterization of*
609 *their cargo and antiviral activity.* Placenta, 2016. **47**: p. 86-95.
610 39. Thery, C., et al., *Isolation and characterization of exosomes from cell culture supernatants and*
611 *biological fluids.* Curr Protoc Cell Biol, 2006. **Chapter 3**: p. Unit 3 22.
612 40. Zicari, S., et al., *Human cytomegalovirus-infected cells release extracellular vesicles that carry viral*
613 *surface proteins.* Virology, 2018. **524**: p. 97-105.
614 41. Consortium, E.-T., et al., *EV-TRACK: transparent reporting and centralizing knowledge in*
615 *extracellular vesicle research.* Nat Methods, 2017. **14**(3): p. 228-232.
616 42. Hurbain, I., et al., *Analyzing Lysosome-Related Organelles by Electron Microscopy.* Methods Mol
617 Biol, 2017. **1594**: p. 43-71.
618 43. Raposo, G., et al., *B lymphocytes secrete antigen-presenting vesicles.* J Exp Med, 1996. **183**(3): p.
619 1161-72.
620 44. Koliha, N., et al., *A novel multiplex bead-based platform highlights the diversity of extracellular*
621 *vesicles.* J Extracell Vesicles, 2016. **5**: p. 29975.
622 45. Polliotti, B.M., et al., *Culture of first-trimester and full-term human chorionic villus explants: role of*
623 *human chorionic gonadotropin and human placental lactogen as a viability index.* Early Pregnancy,
624 1995. **1**(4): p. 270-80.
625 46. Wiklander, O.P.B., et al., *Systematic Methodological Evaluation of a Multiplex Bead-Based Flow*
626 *Cytometry Assay for Detection of Extracellular Vesicle Surface Signatures.* Front Immunol, 2018. **9**:
627 p. 1326.
628 47. Sammar, M., et al., *Expression of CD24 and Siglec-10 in first trimester placenta: implications for*
629 *immune tolerance at the fetal-maternal interface.* Histochem Cell Biol, 2017. **147**(5): p. 565-574.
630 48. Lee, C.Q., et al., *What Is Trophoblast? A Combination of Criteria Define Human First-Trimester*
631 *Trophoblast.* Stem Cell Reports, 2016. **6**(2): p. 257-72.

632 49. Gregory, A.L., et al., *Review: the enigmatic role of endoglin in the placenta.* Placenta, 2014. **35**
633 **Suppl**: p. S93-9.
634 50. Higuchi, T., et al., *Cyclic AMP enhances the expression of an extravillous trophoblast marker,*
635 *melanoma cell adhesion molecule, in choriocarcinoma cell JEG3 and human chorionic villous*
636 *explant cultures.* Mol Hum Reprod, 2003. **9**(6): p. 359-66.
637 51. Wong, F.T.M., C. Lin, and B.J. Cox, *Cellular systems biology identifies dynamic trophoblast*
638 *populations in early human placentas.* Placenta, 2019. **76**: p. 10-18.
639 52. Blaschitz, A., H. Hutter, and G. Dohr, *HLA Class I protein expression in the human placenta.* Early
640 Pregnancy, 2001. **5**(1): p. 67-9.
641 53. Lv, F.J., et al., *Concise review: the surface markers and identity of human mesenchymal stem cells.*
642 Stem Cells, 2014. **32**(6): p. 1408-19.
643 54. Salomon, C., et al., *Exosomal signaling during hypoxia mediates microvascular endothelial cell*
644 *migration and vasculogenesis.* PLoS One, 2013. **8**(7): p. e68451.
645 55. Faye, A., et al., *Evaluation of the placental environment with a new in vitro model of histocultures*
646 *of early and term placentae: determination of cytokine and chemokine expression profiles.*
647 Placenta, 2005. **26**(2-3): p. 262-7.
648 56. Hamilton, S.T., et al., *Human cytomegalovirus-induces cytokine changes in the placenta with*
649 *implications for adverse pregnancy outcomes.* PLoS One, 2012. **7**(12): p. e52899.
650 57. Salomon, C., et al., *Extravillous trophoblast cells-derived exosomes promote vascular smooth*
651 *muscle cell migration.* Front Pharmacol, 2014. **5**: p. 175.
652 58. Pereira, L., et al., *Insights into viral transmission at the uterine-placental interface.* Trends
653 Microbiol, 2005. **13**(4): p. 164-74.
654 59. Pereira, L., et al., *Congenital cytomegalovirus infection undermines early development and*
655 *functions of the human placenta.* Placenta, 2017. **59 Suppl 1**: p. S8-S16.
656 60. Amirhessami-Aghili, N., et al., *Human cytomegalovirus infection of human placental explants in*
657 *culture: histologic and immunohistochemical studies.* Am J Obstet Gynecol, 1987. **156**(6): p. 1365-
658 74.

659 61. Uenaka, M., et al., *Histopathological analysis of placentas with congenital cytomegalovirus*
660 *infection.* Placenta, 2019. **75**: p. 62-67.
661 62. Cantin, R., et al., *Discrimination between exosomes and HIV-1: purification of both vesicles from*
662 *cell-free supernatants.* J Immunol Methods, 2008. **338**(1-2): p. 21-30.
663 63. Nolte-'t Hoen, E., et al., *Extracellular vesicles and viruses: Are they close relatives?* Proc Natl Acad
664 Sci U S A, 2016. **113**(33): p. 9155-61.
665 64. Nagao, K., et al., *Abnormal placental development and early embryonic lethality in EpCAM-null*
666 *mice.* PLoS One, 2009. **4**(12): p. e8543.
667 65. Fast, L.A., et al., *Inhibition of Tetraspanin Functions Impairs Human Papillomavirus and*
668 *Cytomegalovirus Infections.* Int J Mol Sci, 2018. **19**(10).
669 66. Viswanathan, K., et al., *Quantitative membrane proteomics reveals a role for tetraspanin enriched*
670 *microdomains during entry of human cytomegalovirus.* PLoS One, 2017. **12**(11): p. e0187899.
671

672 **FIGURE LEGENDS**

673

674 **Figure 1: Placental histoculture set-up and characterization.**

675 A) Pipeline of placental histoculture model. B) β-HCG measurements in histoculture
676 supernatant. For each placental histoculture, β-HCG measurement was realized in the
677 supernatant between days 3-5 (measure 1) and days 10-12 (measure 2). **** *p<0.0001* by
678 paired *t*-test (n=21 independent histocultures). C) Cross sections of immunohistochemistry
679 and hematoxylin staining of placental villi from histoculture at day 14, observed by bright field
680 microscope. a- Isotype control; b- Cytokeratin 7; c- PLAP; d- Vimentin. Image representative
681 from at least three independent experiments. Scale bar = 50 μm.

682

683 **Figure 2: sEV preparation pipeline and flow cytometry analysis.**

684 A) Pipeline of sEV preparation from placental histoculture collected medium. B) Flow
685 cytometry standardization on fluorescent-FITC beads (160 nm, 200 nm, 240 nm and 500 nm).
686 Each population size was defined on SSC granularity and FITC fluorescence parameters. The
687 black rectangle indicates the gating strategy on small bead populations (160nm and 200nm).
688 The dashed line represents the threshold for the detection of sEVs. C) Representative analysis
689 of one placental sEV preparation gated on small events as described above. In this example,
690 89% of events were below 200nm. All data were analyzed with FlowJo software (BD).
691
692 **Figure 3: Nanoparticle tracking analysis of sEV prepared from placental explants.**
693 A) Individual analyses of mode size (nm) of four independent placental sEV preparations.
694 Histograms represent mean of mode size ± SEM from three independent measurements
695 (represented by individual dots) for each independent preparation. B) and C) Representative
696 analyses of sEV size and concentration of two sEV samples (respectively, #37 in B and #38 in
697 C).
698
699 **Figure 4: Electron and immuno-electron microscopy characterization of placental sEVs.**
700 A) Placental sEVs observed by TEM from two independent experiments. sEVs are indicated by
701 black arrows. Scale bar = 100 nm. B) Mean size and min/max of placental sEVs for two
702 independent experiments. Placental sEV size were measured manually with iTEM measure
703 tool. C) Frequency distribution analysis of placental sEV size. Each bar of the histogram
704 represents the mean ± SEM of the relative frequency per bin (bin width = 20 nm) of two
705 independent experiments. Total sEV count was 172 for #31 and 208 for #32. D) Placental sEV
706 were immunogold-labelled for CD63, revealed with Protein A-gold particle of 10 nm diameter
707 and observed by TEM. Scale bar = 100 nm (n = 2). E) Percentage of placental sEV positive for

708 CD63 (at least one bead counted per sEV) for two independent experiments. Total sEV count
709 was 189 for #31 and 263 for #32.
710
711 **Figure 5: Placental sEV surface protein analysis.**
712 A) Surface expression level of several proteins of sEVs, based on the multiplex flow cytometry
713 Macsplex exosome kit assay. Each bar of the histogram represents the mean ± SEM calculated
714 from 6 independent experiments, expressed in Arbitrary Units (A. U.) for different sEV markers
715 indicated on the X axis. The dashed line represents the detection limit of the test (defined by
716 the two first controls on the left of the histogram). B) Representative western blot analysis
717 against CD63 performed on two independent sEV preparations (#33 and #35). CD63 appears
718 as a smear, since the non-reducing conditions of the western blot preserve its rich glycosylated
719 pattern. MW = molecular weight.
720
721 **Figure 6: Impact of hCMV infection on placental histocultures.**
722 A) Titration of hCMV genome copies released in histoculture supernatant at day 11, *i.e.* after
723 two medium changes and renewals. On the graph is indicated the median with 95% CI. n=12
724 independent experiments. B) Representative examples of immuno-histochemistry performed
725 against hCMV IE antigen at day 14 on sections of placental villi, counterstained with
726 hematoxylin. Scale bar = 50 μm. C) Comparison of the explant weight at the end-point of the
727 placental histocultures, performed for twelve independent experiments. Each of the placental
728 explants were pooled per condition and weighted (NI = non-infected). Statistical analysis of
729 explant weight variation between the two conditions was performed by Wilcoxon paired t test
730 on GraphPad Prism 8 software and showed no significant difference (ns; *p=0,3804*). D)
731 Comparison of the β-HCG secretion in explant supernatants was performed between non-

732 infected (NI) *versus* hCMV-infected placenta, measured with the same timeline as presented
733 in Figure 1A. ns, non-significant (*p=0.9697* for measure 1; *p=0,5693* for measure 2) by
734 Wilcoxon paired *t*-test. n=12 independent experiments. E) Cross sections of
735 immunohistochemistry and hematoxylin staining of hCMV infected placental villi from
736 histoculture at day 14, observed by bright field microscope. a- Isotype control; b- Cytokeratin
737 7; c- PLAP; d- Vimentin. Image representative from at least three independent experiments.
738 Scale bar = 50 μm.
739
740 **Figure 7: Placental sEV isolation and characterization upon hCMV infection.**
741 A) Comparison of the yield of sEV prepared per mg of placental tissue upon sEV preparation
742 between non-infected (NI) *versus* hCMV-infected placental explants. Yield is expressed in sEV
743 number/mg tissue, obtained from nine independent experiments. ns, non-significant by
744 Wilcoxon *t*-test. B) Western blot analysis against CD63 in sEVs prepared from non-infected
745 (NI) or infected (hCMV) placental explants. This result is representative for at least three
746 independent experiments. CD63 appears as a smear since the non-reducing conditions of the
747 western blot preserves its rich glycosylated pattern. MW = molecular weight. C) Placental sEV
748 isolated from non-infected (NI) *versus* infected (hCMV) placental explants, obtained by TEM.
749 These pictures are representative of two independent experiments. Scale bar = 100 nm. D)
750 Frequency distribution analysis of placental sEV size, compared between non-infected (NI)
751 *versus* infected (hCMV) placental explants. Each bar of the histogram represents the mean ±
752 SEM of the relative frequency per bin (bin width = 20 nm) of two independent experiments.
753 Placental sEV size were measured manually with iTEM measure tool. Total sEV count was 172
754 and 208 for the NI replicates; 176 and 185 for the hCMV replicates. Statistical analysis of the
755 distribution between the two conditions was performed by nested *t*-test and showed no

756 significant difference (*p=0.8814*). E) Mean size ± SEM of placental sEV purified from non-
757 infected (NI) or infected (hCMV) placental explants, calculated from the experiments
758 presented in (D). ns, non-significant by nested *t*-test (*p=0.8871*). F and G) Representative
759 pictures of IEM analysis of placental sEV using antibodies against CD63 (gold bead size = 10
760 nm), purified from non-infected (NI; F) *versus* infected (hCMV; G) placental explants (n = 2).
761 Scale bar = 100 nm. H) Percentage of placental sEV positive for CD63 (at least 1 bead counted
762 per sEV) for two independent experiments. Total sEV count was 189 and 263 for sEV isolated
763 from non-infected placental explants; 143 and 594 for sEV isolated from infected explants. ns,
764 non-significant by nested *t*-test. I) Surface expression level of different proteins of sEV isolated
765 from non-infected (NI) *versus* infected (hCMV) placental explants, based on the multiplex flow
766 cytometry Macsplex exosome kit assay. Results are represented by a heat-map, calculated
767 from 3 independent experiments for different sEV markers indicated on the left column. Blue
768 intensity is proportional to the level expression calculated in Arbitrary Units (A. U.), indicated
769 on the right of the heat-map. *p <0.0001* by 2-way ANOVA for "Infection" factor. Bonferroni
770 post-hoc comparison test indicated significant increase for CD81 (**, p=0.0223*) and CD326 (***,*
771 *p=0.0029*) for hCMV compared to non-infected (NI) conditions.
772
773 Word count: 9007.

Bergamelli et al, Fig 1

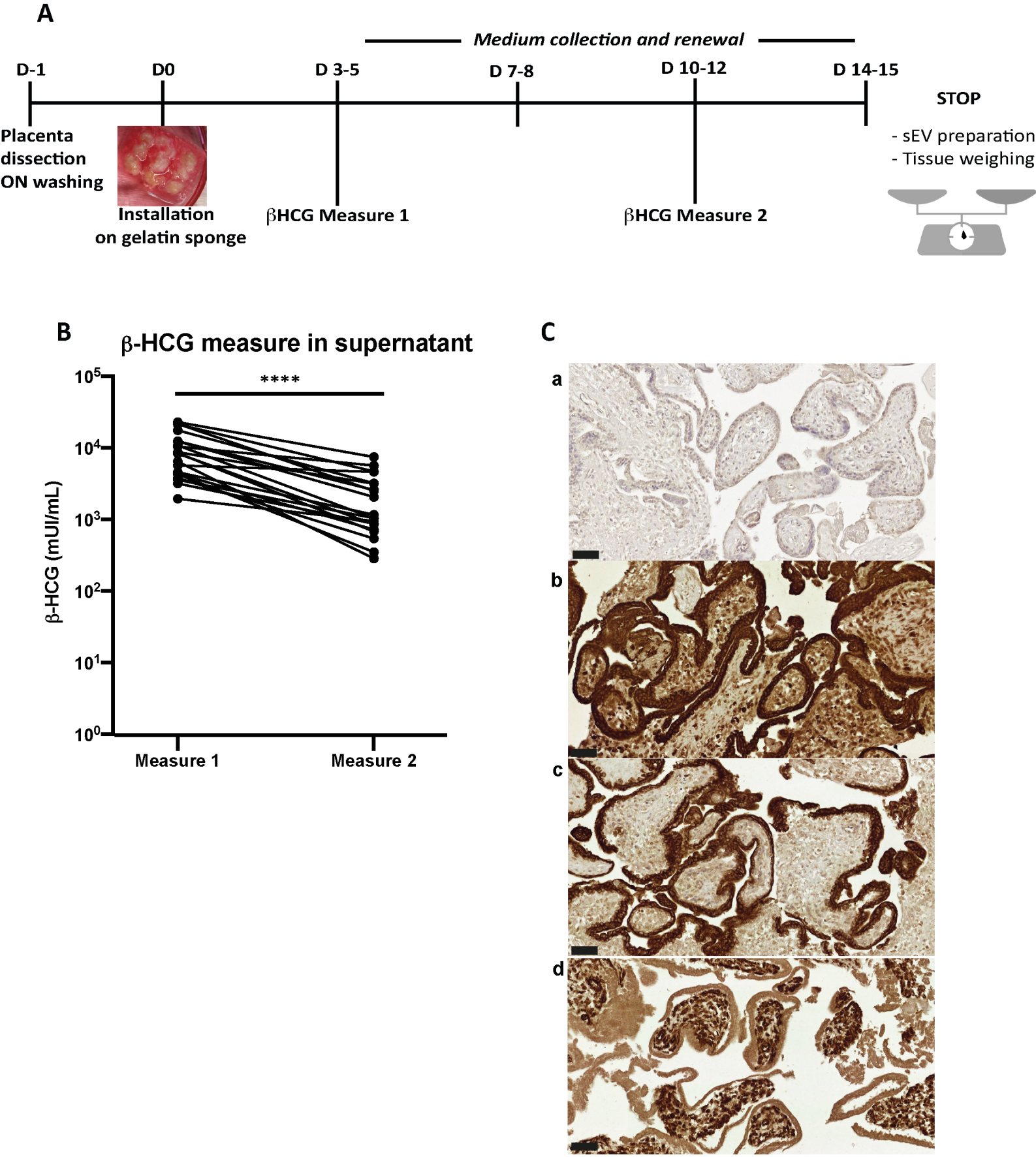

Bergamelli et al, Fig 2

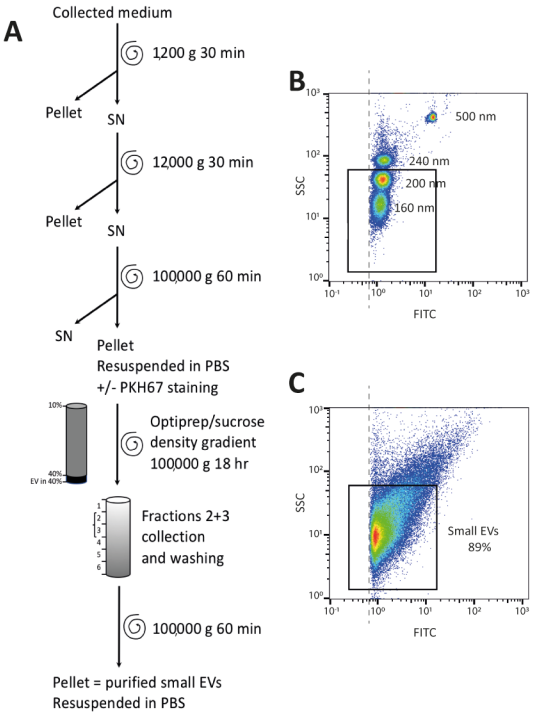

Bergamelli et al, Fig 3

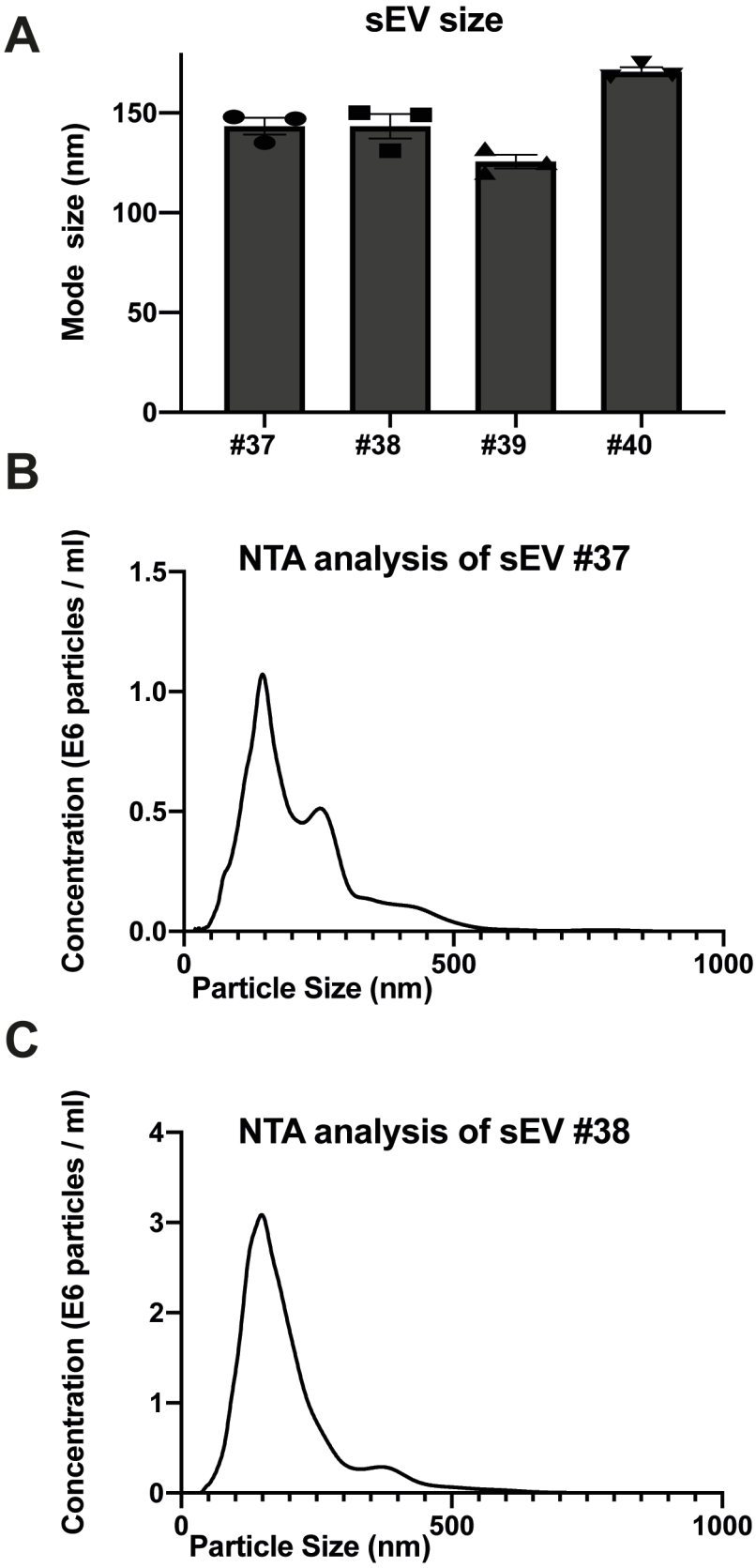

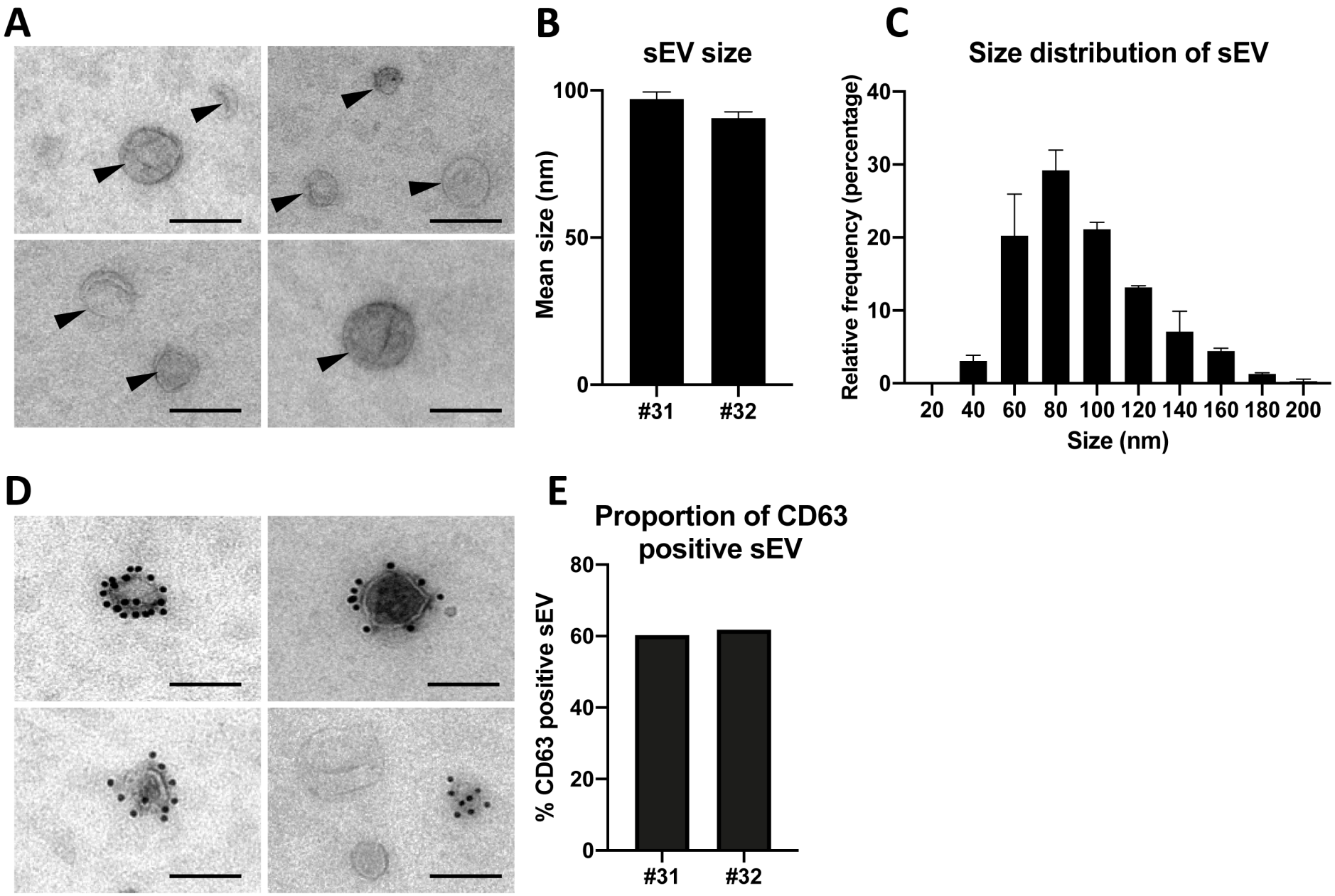

Bergamelli et al, Fig 4

A

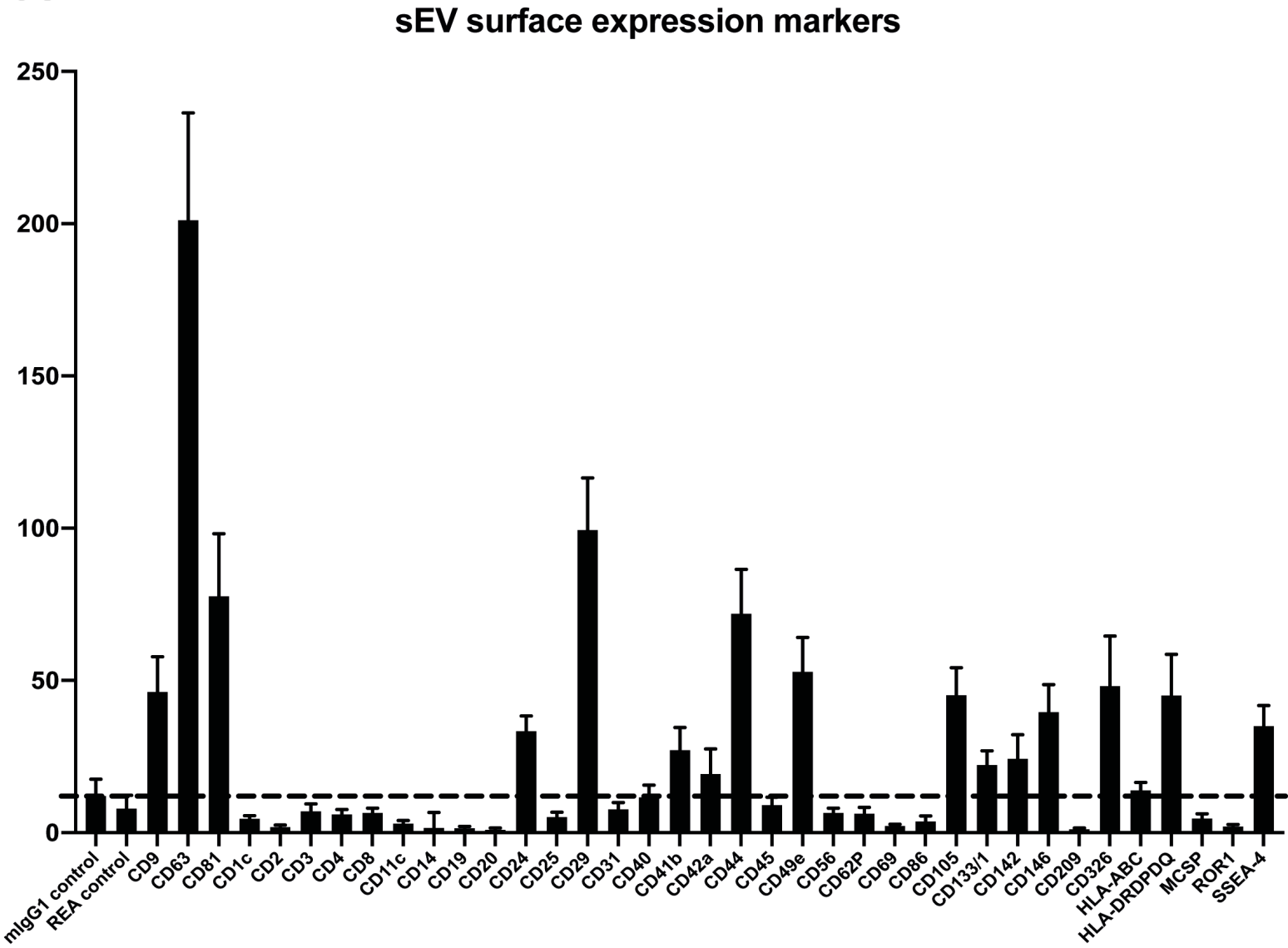

B

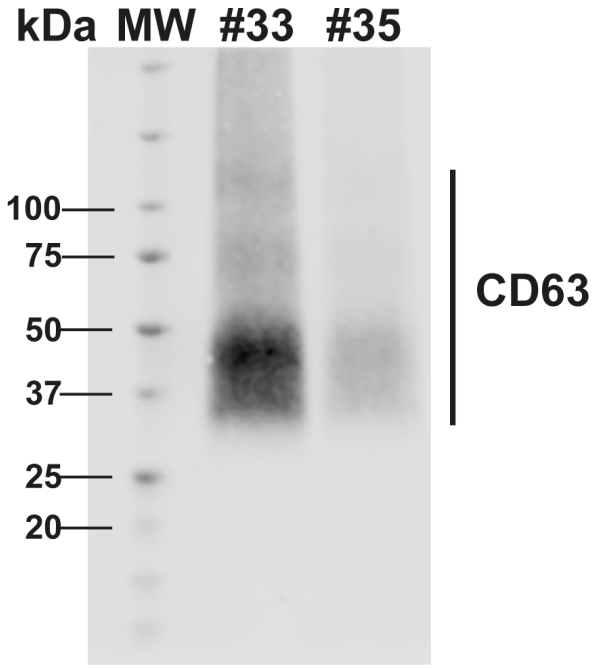

Bergamelli et al, Fig 5

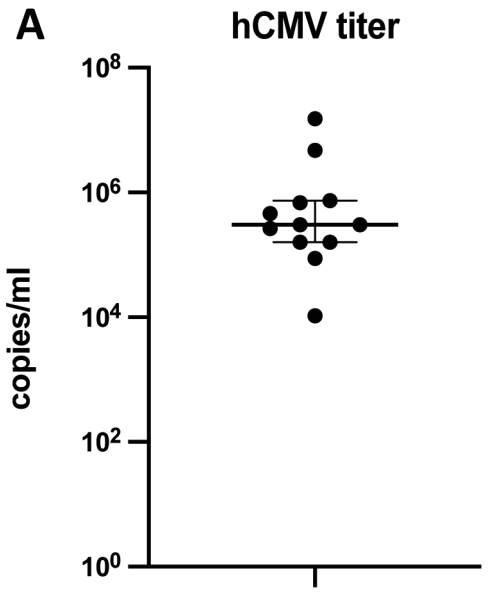
A
hCMV titer
copies/ml
10^8
10^6
10^4
10^2
10^0

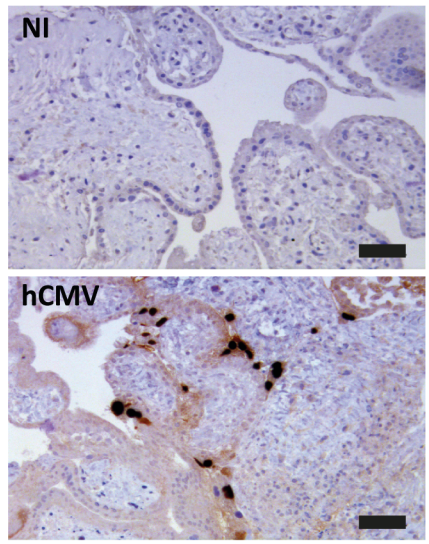
B
NI
hCMV

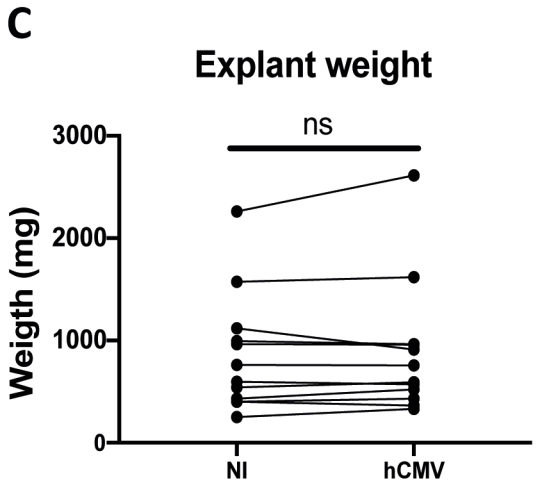
C
Explant weight
ns
Weigth (mg)
3000
2000
1000
0
NI
hCMV

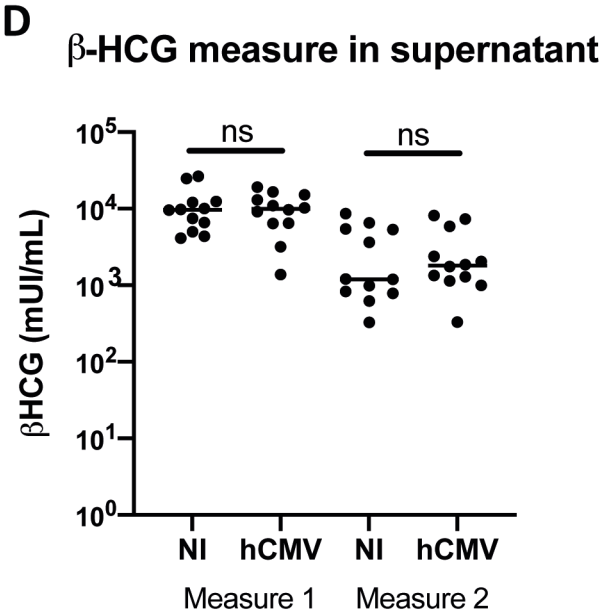
D
β-HCG measure in supernatant
ns
ns
βHCG (mUI/mL)
10^5
10^4
10^3
10^2
10^1
10^0
NI
hCMV
NI
hCMV
Measure 1
Measure 2

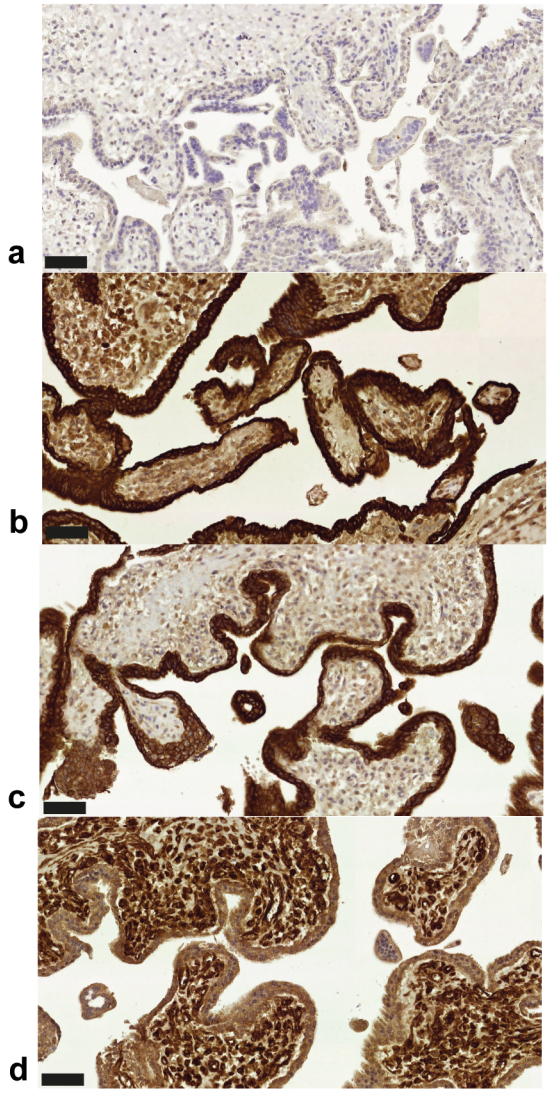
E
a
b
c
d

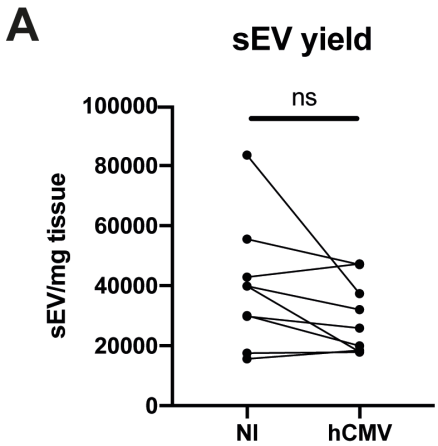
A
sEV yield
ns
sEV/mg tissue
100000
80000
60000
40000
20000
0
NI
hCMV

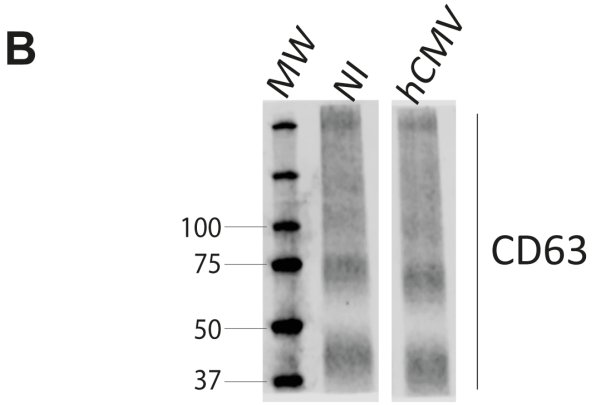
B
MW
NI
hCMV
100
75
50
37
CD63

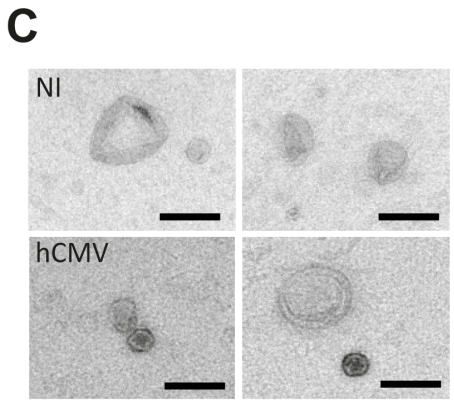
C
NI
hCMV

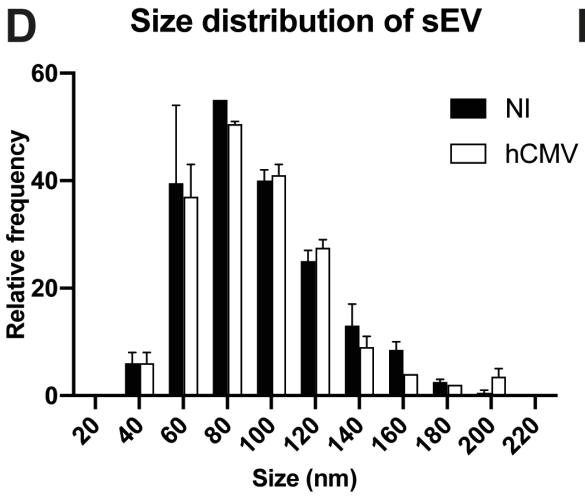
D
Size distribution of sEV
Relative frequency
60
40
20
0
NI
hCMV
20
40
60
80
100
120
140
160
180
200
220
Size (nm)

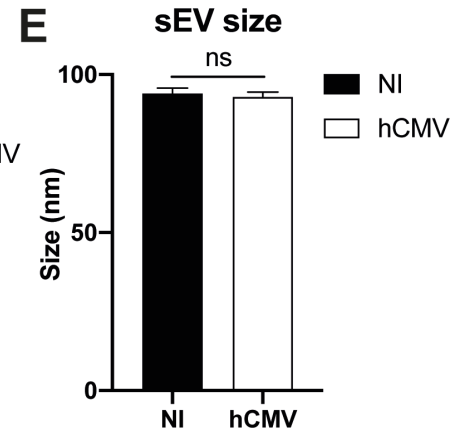
E
sEV size
ns
Size (nm)
100
50
0
NI
hCMV
NI
hCMV

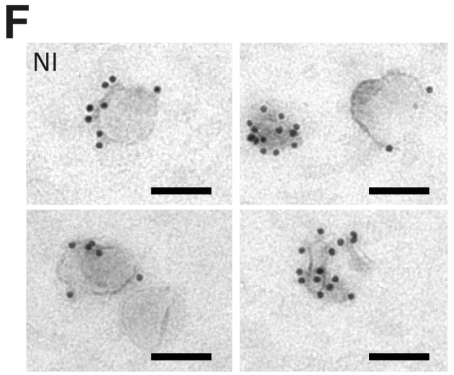
F
NI

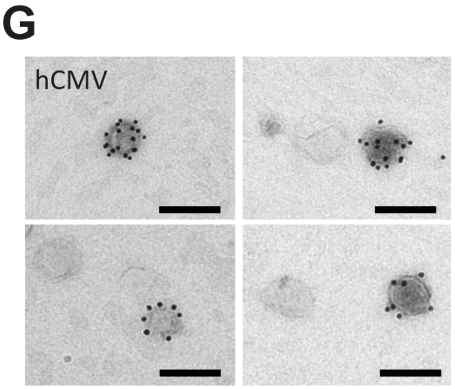
G
hCMV

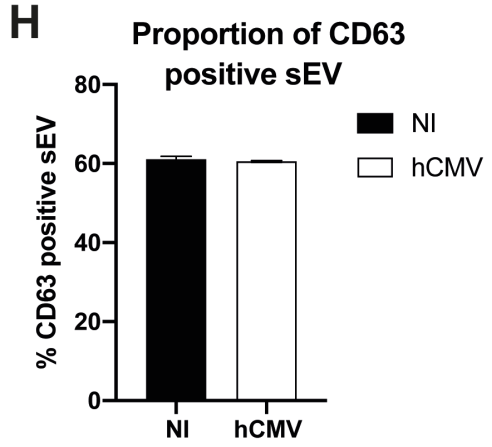
H
Proportion of CD63 positive sEV
% CD63 positive sEV
80
60
40
20
0
NI
hCMV
NI
hCMV

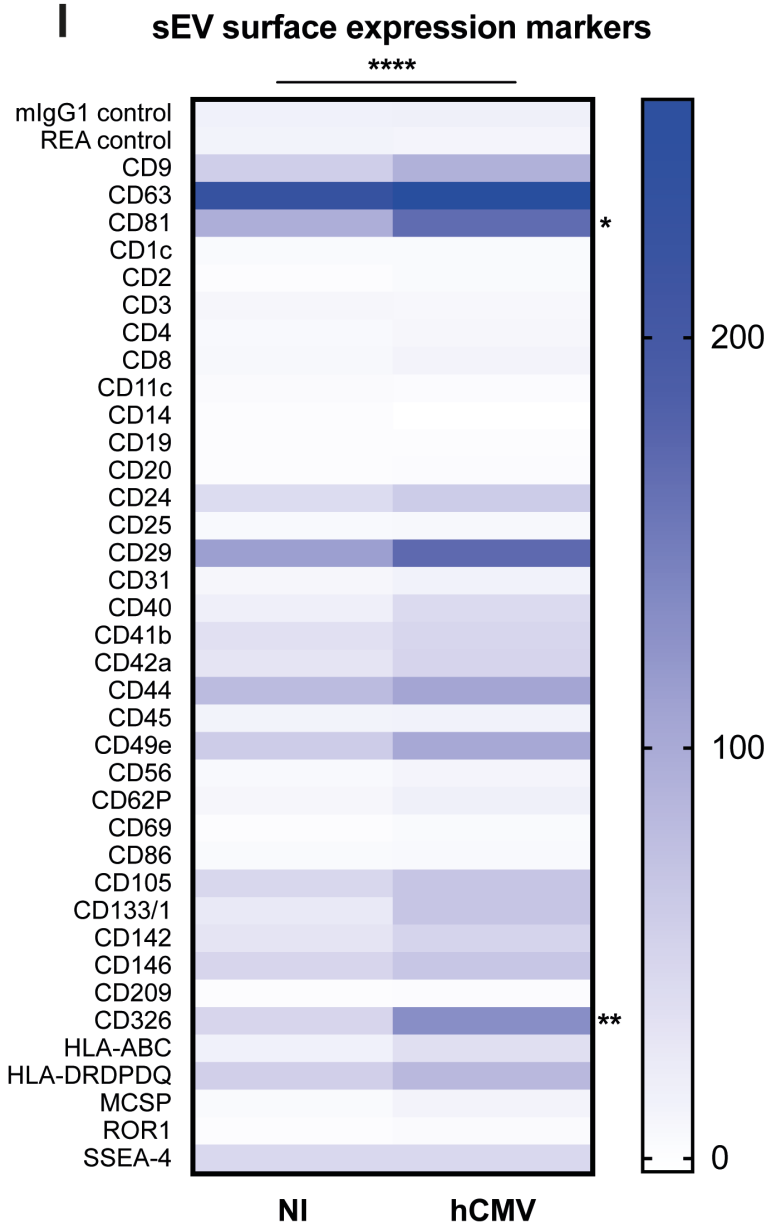
I
sEV surface expression markers
****
mIgG1 control
REA control
CD9
CD63
CD81
CD1c
CD2
CD3
CD4
CD8
CD11c
CD14
CD19
CD20
CD24
CD25
CD29
CD31
CD40
CD41b
CD42a
CD44
CD45
CD49e
CD56
CD62P
CD69
CD86
CD105
CD133/1
CD142
CD146
CD209
CD326
HLA-ABC
HLA-DRDPDQ
MCSP
ROR1
SSEA-4
*
**
200
100
0
NI
hCMV